Korean Journal of Remote Sensing, Vol.24, No.1, 2008, pp.57~64

A Comparative Study of 3D DWT Based Space-borne Image Classification for Differnet Types of Basis Function

Hee-Young Yoo*†, Kiwon Lee, and Byung-Doo Kwon***

*Department of Earth Science Education, Seoul National University, Shillim-dong, Kwanak-gu, 151-742, Seoul, Korea
**Department of Information System Engineering, Hansung University, Samsun-dong, Sungbuk-gu, 136-792, Seoul, Korea

Abstract : In the previous study, the Haar wavelet was used as the sole basis function for the 3D discrete wavelet transform because the number of bands is too small to decompose a remotely sensed image in band direction with other basis functions. However, it is possible to use other basis functions for wavelet decomposition in horizontal and vertical directions because wavelet decomposition is independently performed in each direction. This study aims to classify a high spatial resolution image with the six types of basis function including the Haar function and to compare those results. The other wavelets are more helpful to classify high resolution imagery than the Haar wavelet. In overall accuracy, the Coif4 wavelet has the best result. The improvement of classification accuracy is different depending on the type of class and the type of wavelet. Using the basis functions with long length could be effective for improving accuracy in classification, especially for the classes of small area. This study is expected to be used as fundamental information for selecting optimal basis function according to the data properties in the 3D DWT based image classification.

Key Words : 3D DWT, Basis function, Classification, High-resolution imagery.

1. Introduction

Mathematical transformations have been applied to the signals to obtain further information that is not readily available in raw signal. Among a number of transforms, wavelet transform is capable of providing both the location and frequency information simultaneously. The discrete wavelet transform (DWT) has been extensively used in 2D image processing techniques: compressing large-sized image sets, reducing the noise of imagery, fusing and analyzing multi-scale images (Solbø and Eltoft, 2004; Boucheron and Creusere, 2005; Koger *et al.*, 2003; Plaza *et al.*, 2005; Yunhao *et al.*, 2006; Tso and Olsen, 2005).

Most remotely sensed images except for some radar images do not contain information regarding subsurface, since the used waves cannot penetrate into surface. Remotely sensed imagery is basically two dimensional data. If several images were acquired at the same location over multiple spectral bands or temporal bands, remotely sensed imagery

Received 1 February 2008; Accepted 22 February 2008.
† Corresponding Author: Hee-Young Yoo (skyblue1@snu.ac.kr)

also could be considered a kind of 3D data even though image is not 3D data in the strict sense of the word. 3D DWT could be accordingly applied to the three dimension image data having multiple bands. In this instance, depth is substituted for information of spectral domain.

Yoo *et al.* (2007) applied 3D DWT to classifying satellite images, and their results were compared with those of traditional classification including the 2D DWT based classification. Accuracy assessment demonstrated that the 3D DWT based classification is more effective for land-cover classification than the 2D DWT based method as well as the traditional pixel based method. The Haar wavelet was used as the sole basis function for the 3D DWT decomposition because the number of bands is too small to decompose remotely sensed images with other basis functions. However, it is possible to employ other basis functions primarily used in 2D image processing for wavelet decomposition in horizontal and vertical directions, such as the Daubechies, Coiflets and Symlets functions, because wavelet decomposition is independently performed in each direction. In this study, maximum likelihood classifications with the six types of basis functions are performed with the image, training and reference data used in the previous experiments (Yoo *et al.*, 2007). These results are compared with the case of the Haar wavelet.

2. Methodology

1) 3D Discrete Wavelet Transform

The basic idea of wavelet transform is to represent signal as a superposition of wavelets. DWT is based on sub-band coding to yield a fast computation of wavelet transform. The DWT decomposition can be implemented using two channel filter banks composed of a low-pass and a high-pass filter, and each filter bank is then sampled at a half rate of the frequency at the upper level. The signal can be represented in terms of these coefficients at level J as

$$f(x) = \sum_k c_{Jk}\phi_{Jk}(x) + \sum_{j=1}^{J}\sum_k d_{jk}\psi_{jk}(x) \qquad (1)$$

where c_{jk} are the scaling coefficients and d_{jk} are the wavelet coefficients. The first term in Eq. (1) gives the low-resolution approximation of the signal while the second term gives the detailed information at different resolutions from the original down to the current resolution (Pajares and Cruz, 2004).

3D DWT expands the 1D wavelet theory into three dimensions and decomposes data not only in row and column directions but also in depth direction (Yoo *et al.*, 2007). In terms of the wavelet space decomposition, 3D DWT can be constructed by a tensor product by

$$\begin{aligned} V^3 &= (L^x \oplus H^x)\otimes(L^y \oplus H^y)\otimes(L^z \oplus H^z) \\ &= L^x\otimes L^y\otimes L^z \oplus L^x\otimes L^y\otimes H^z \\ &\quad \oplus L^x\otimes H^y\otimes L^z \oplus H^x\otimes L^y\otimes L^x \\ &\quad \oplus L^x\otimes H^y\otimes H^z \oplus H^x\otimes L^y\otimes H^z \\ &\quad \oplus H^x\otimes H^y\otimes L^z \oplus H^x\otimes H^y\otimes H^z \end{aligned} \qquad (2)$$

where $\oplus$ and $\otimes$ denote the space direct sum and direct multiplication, respectively. H^λ and L^λ represent the high and low-pass directional filters along the direction of λ-axis, where $\lambda = \{x, y, z\}$ (Chen and Ning, 2004). 8 sub-bands are formed from 3D DWT. Each sub-band obtained through two frequency filters is named by directions, frequency filter passed in: LLL, LLH, LHL, HLL, LHH, HLH, HHL, and HHH. 3D DWT could be applied to the three dimensional image data having multiple bands. Fig. 1 shows the result of the 3D DWT decomposition using real multi-band image.

2) Properties of Basis Functions

Wavelets are used as basis functions in representing

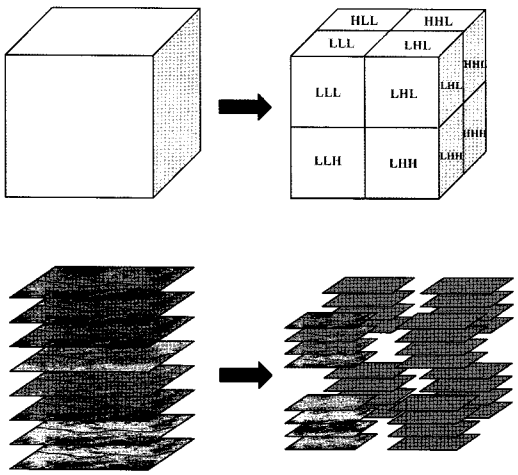

Fig. 1. Example of 3D wavelet decomposition in one level using real satellite image.

signals, like sinusoidal function in Fourier analysis. Wavelets are functions that satisfy certain requirements; to integrate to zero, waving above and below the X-axis, to insure quick and easy calculation of the direct and inverse wavelet transform. There are different types of wavelet families whose qualities vary according to several criteria. The main criteria are the support of forward and inverse transform, the symmetry, the number of vanishing moments, the regularity, the existence of a scaling function and the orthogonality or the biorthogonality. The support of forward and inverse transform means the speed of convergence to 0 of the function when the time t or the frequency ω goes to infinity. The symmetry is useful to avoid de-phasing in image processing. The number of vanishing moments for ψ or for ϕ is useful for compression purposes. ψ and ϕ means denotes the function and scaling function, respectively. The regularity, which is useful for getting nice features, means the smoothness of the reconstructed signal or image and is for the estimated function in nonlinear regression analysis. The existence of a scaling function and the orthogonality or the biorthogonality of the resulting analysis are associated with two properties that allow fast algorithm and space-saving coding (Daubechies, 1992).

We used the six different basis functions for wavelet decomposition in horizontal and vertical directions: Haar, Daubechies 4(Db4), Symlets 4 (Sym4), Coiflets 4 (Coif4), Biorthogonal 3.5(Bior 3.5) and 3.9 (Bior 3.9) (Fig. 2). The used basis functions in this study are explained with these criteria in detail (Table 1).

The Haar wavelet, the simplest and shortest type of orthonormal wavelet was proposed by Alfred Haar in 1909 (Eq. (3)). The disadvantage of the Haar wavelet

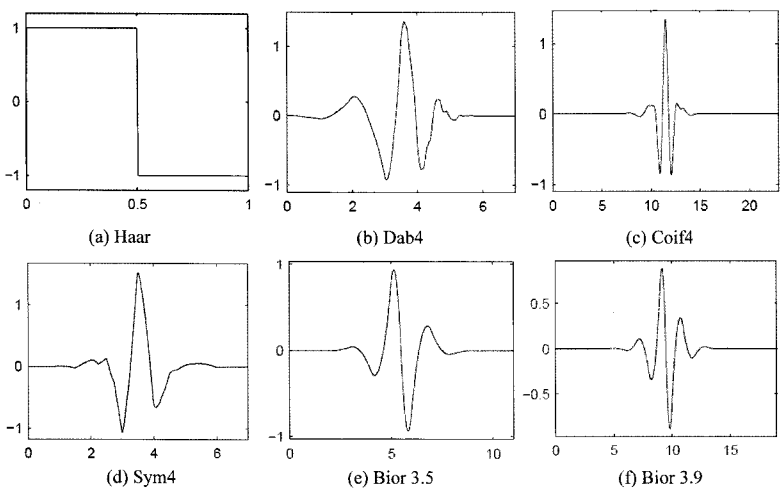

Fig. 2. Six types of basis functions (Matlab Wavelet Toolbox User's Guide).

Table 1. Summary of wavelet families and associated properties (Matlab Wavelet Toolbox User's Guide)

Property	haar	dbN	symN	coifN	biorNr.Nd
Arbitrary regularity		●	●	●	●
Compactly supported orthogonal	●	●	●	●	
Compactly supported biorthogonal					●
Symmetry	●				●
Asymmetry		●			
Near symmetry			●	●	
Arbitrary number of vanishing moments		●	●	●	●
Vanishing moments for Φ				●	
Existence of Φ	●	●	●	●	●
Orthogonal analysis	●	●	●	●	
Biorthogonal analysis	●	●	●	●	●
Exact reconstruction	●	●	●	●	●
FIR filters	●	●	●	●	●
Continuous transform	●	●	●	●	●
Discrete transform	●	●	●	●	●
Fast algorithm	●	●	●	●	●

is that it is not continuous and therefore not differentiable.

$$f(x) = \begin{cases} 1 & 0 \le x < 1/2, \\ -1 & 1/2 \le x < 1, \\ 0 & \text{otherwise.} \end{cases} \quad (3)$$

The Db4 is a type of Daubechies wavelets. Daubechies wavelets are the most popular wavelets, which represent the foundations of wavelet signal processing and are used in numerous applications. In the db*N*, *N* is the order. The number of vanishing moments of ψ is *N*. Most Daubechies wavelets are not symmetrical unlike the other wavelets. For some, the asymmetry is very pronounced. The regularity increases with the order and the analysis is orthogonal.

The Sym4 is a type of Symlets wavelets. Symlets are only near symmetric however they are more symmetrical than Daubechies wavelets. Symlets have some properties similar to those of Daubechies wavelets.

The Coif4 belongs to Coiflet wavelets. Coiflets are near symmetric same as Symlets however they are much more symmetrical than the *dbN*. The most important thing in Coiflets is that they are compactly supported wavelets with highest number of vanishing moments for both ψ and ϕ for a given support width and the length of wavelet is the longest among the other basis functions.

Meanwhile, The biorthogonal wavelet pairs (*biorNr.Nd*) are compactly supported biorthogonal spline wavelets and symmetrical. *Nr* and *Nd* mean the orders. The two wavelets, instead of just one are used in the analysis in case of biorthogonal wavelets. Bior 3.5 and Bior 3.9 are used for this study. Two basis functions have all same properties but only the order is different each other.

3. Classification of 3D DWT Coefficients

The procedure of this study is shown in Fig. 3. First, bands are arranged in the order of wavelength and the number of data in row, column and depth directions should be then a power of two to

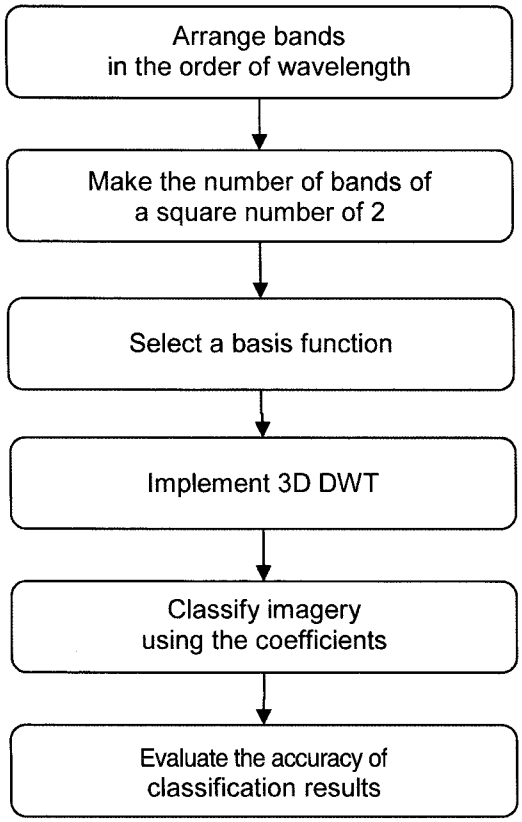

Fig. 3. Flow chart of classification procedure based on 3D DWT.

implement 3D DWT using multi-spectral imagery. The next step is to select a basis function and to implement 3D DWT with the selected wavelet for row and column directions and with the Haar wavelet for band direction in 1-level. Lastly, we classify the image using the 3D wavelet coefficients of the pixels at original resolution and then evaluate the results. The maximum likelihood classifier is applied to the image data for this experiment. Among the 3D DWT sub-bands, only the LLL and the LLH bands are used for the classification. We mean to classify remotely sensed images considering neighborhood pixels as well as individual pixels. Most land-cover maps provided officially are usually prepared by reclassifying and simplifying the raw classification results. An excess of complicated spatial information interferes with making land-cover map because the other sub-bands highlight noise and details, which are less important for making a land-cover map. Using only the LLL and LLH bands could produce greater in classification accuracy than using all sub-bands.

The Ikonos imagery in Hobart, Australia used for this study is one of ISPRS dataset collections (http://www.isprs.org/data/index.html) and is composed of red, green, blue, near infrared bands (4m). The training and reference data sets are indicated on the test image in Fig. 4. The reference data is divided into residential area, forest, water, commercial area and grass (Fig. 4(b)). The number of reference pixels by class is 142277 in residential area, 42546 in forest, 84391 in water, 29224 in commercial area and 1892 in grass, respectively. This reference set was collected from the image by visual check because the classes in high resolution image can be divided visually. The training data set is obtained 10% random sampling of each reference data set (Fig. 4 (a)). The explanation between the class and the color is given in the right part of the reference data set.

Fig. 5 illustrates classification results according to the basis function. The six images in Fig. 5 result from classification with the Haar, Db4, Coif4, Sym4, Bior 3.5 and Bior 3.9 wavelets, respectively. The results are similar but small features in the water class, which are presumed to be ships, are exaggerated when the wavelets other than the Haar wavelet are used. Differences between the results depending on wavelet type are difficult to check visually. The following section discusses accuracy assessments for evaluating these results quantitatively.

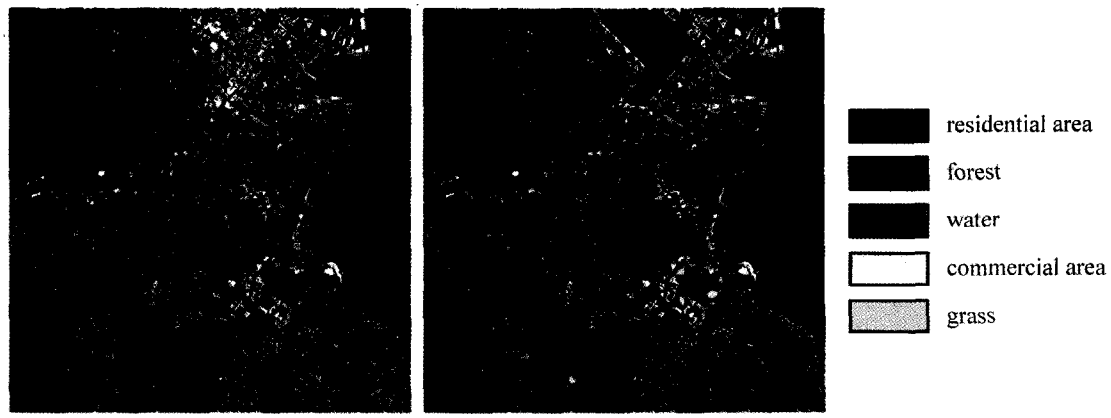

Fig. 4. Training and reference data sets for supervised classification with class indexes: (a) training data set, (b) reference data set.

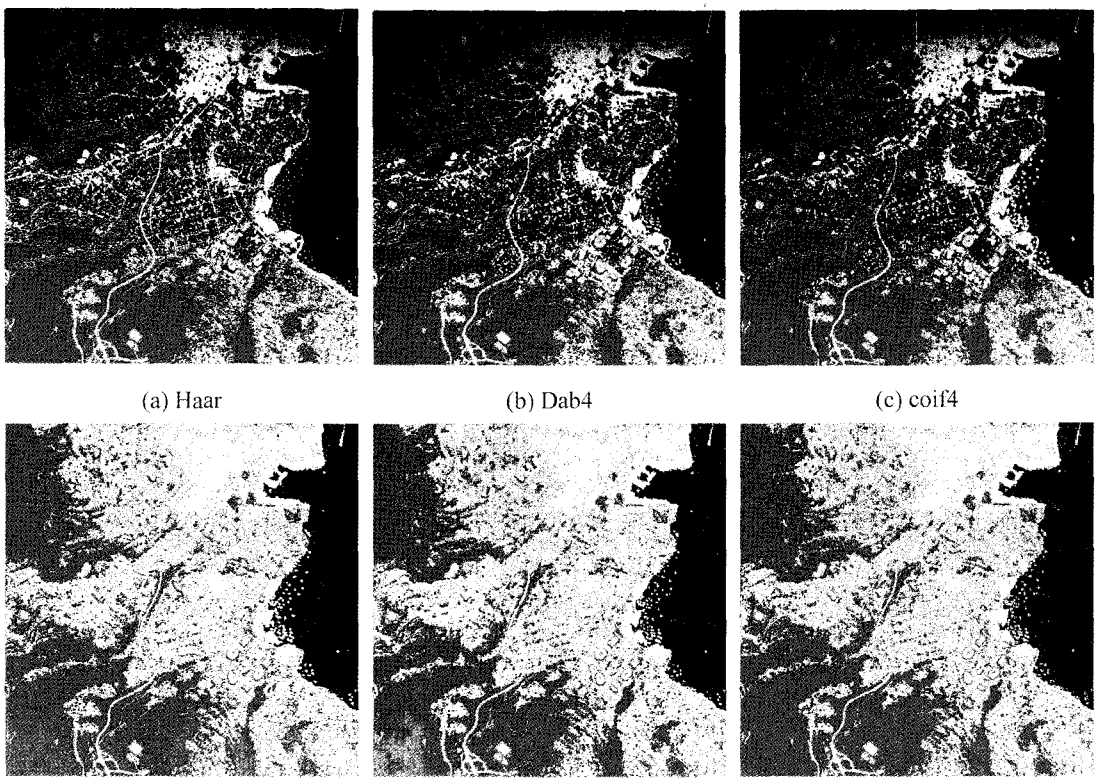

Fig. 5. Comparison of classification results according to basis function. (a) Haar wavelet, (b) Db4 wavelet. (c) coiflet 4 (d) Symlet 4 (e) Biorthogonal 3.5 and (f) Biorthogonal 3.9.

4. Accuracy Assessment

To evaluate the capability of basis functions linked with the 3D DWT classification scheme, the confusion matrixes are presented. Table 2 presents the overall accuracies and the kappa coefficients for all basis functions. For classifying high-resolution imagery, the other wavelets are more helpful than the Haar wavelet. Accuracy of the Haar wavelet, measured to be 86.1267%, is the lowest. The percentages of classification accuracies using the other wavelets are greater than that of the Haar wavelet in all the cases. A significant increase in accuracy is observed for the Coif4 wavelet, from 86.1267% to 89.1373%. The Bior 3.9 wavelet also exhibited higher accuracy (88.0676%). In general, the longer wavelets demonstrate greater accuracy but shorter wavelets have lower accuracy. The Coif4 wavelet, which is the longest wavelet, has the greatest overall accuracy. Although, the length of the Db4 wavelet is very short, this wavelet has relatively greater accuracy. This exception would be quite relevant that the Daubechies wavelets are asymmetrical.

In order to determine accuracy by class, the user's accuracy is presented in Table 3 according to each wavelet. The user's accuracy is computed by dividing the number of correctly classified pixels in each category by the total number of pixels that are classified into the category. This is a measure of commission error and indicates the probability that a pixel classified into a given category actually represents that category on the ground (Lillesand and Kiefer, 2000). In the other classes, except for the grass class, the user's accuracy using the other basis functions are similar to or slightly greater than that of the Haar wavelet. However, the user's accuracy in the grass class improves greatly. In the case of the Haar wavelet, the user's accuracy of the grass class is very low (25.46%). Meanwhile, accuracies improve when the other wavelets are used: Db4, 65.97%; Coif4, 65.57%; Sym4, 56.32%; Bior 3.5, 64.48%; Bior 3.9, 66.60%.

Table 2. Overall accuracy (in percent) and kappa coefficient of classification results depending on the type of basis function

	overall accuracy	kappa coefficient
Haar	86.1267	0.8043
Db4	87.7556	0.8258
Coif4	89.1373	0.8442
Sym4	87.5368	0.8226
Bior 3.5	87.7815	0.8262
Bior 3.9	88.0676	0.8300

Table 3. Comparison of user's accuracy of each class according to basis function (in percent)

	residential	forest	water	commercial	grass
Haar	96.46	91.30	100.00	46.71	25.46
Db4	96.66	91.34	100.00	48.53	65.97
Coif4	96.55	92.31	100.00	52.13	65.57
Sym4	96.45	89.43	100.00	49.34	56.32
Bior 3.5	96.69	91.02	100.00	48.81	64.48
Bior 3.9	96.66	91.14	100.00	49.48	66.60

The improvement of classification accuracy is different depending on the class type as well the wavelet function-type used. The user's accuracies in the residential area and in the forest class are lower, although overall accuracy using the Sym4 wavelet is higher than that of the Haar wavelet. The accuracy improvement of the Coif4 wavelet is the most conspicuous in the forest and commercial area classes. The Bior 3.5 wavelet is more effective in the residential area class, whereas the Bior 3.9 wavelet is the most useful basis function for the grass class.

5. Conclusions

In this study, the classification using the six

different basis functions is conducted and the results are compared by quantitative accuracy evaluation. Overall accuracy improves slightly when the wavelets other than the Haar wavelet are used in horizontal and vertical directions. Classification accuracy is usually greater when the length of basis function is longer. However, the Db4 wavelet is an exceptionally effective basis function for the 3D DWT-based classification even though the length of Db4 is very short. The user's accuracy according to each class suggests that the basis functions other than the Haar wavelet show improvement in the grass class. The other wavelets perform better than the Haar wavelet for the classification of high resolution imagery and improvement in classification accuracy depends on the class type, especially, in the classes covering very small areas. This study is expected to be fundamental for selecting the optimal basis function according to the data properties in the 3D DWT based image classification, later on.

Acknowledgement

This research was partly supported by a grant (07KLSGC03) from Cutting-edge Urban Development - Korean Land Spatialization Research Project funded by Ministry of Construction & Transportation of Korean government.

References

Boucheron, L. E. and C.D. Creusere, 2005. Lossless wavelet-based compression of digital elevation maps for fast and efficient search and retrieval, *Geoscience and Remote Sensing, IEEE Transactions on*, 43(5): 1210-1214.

Chen, Z. and R. Ning, 2004. Breast volume denoising and noise characterization by 3D wavelet transform, *Computerized Medical Imaging and Graphics*, 28(5): 235-246.

Daubechies, I., 1992. Ten lectures on wavelets, *CBMS, SIAM*, 61: 194-202.

Koger, C. H., L.M. Bruce, D. R. Shawa, and K.N. Reddyc, 2003. Wavelet analysis of hyperspectral reflectance data for detecting pitted morningglory (Ipomoea lacunosa) in soybean (Glycine max), *Remote Sensing of Environment*, 86(1): 108-119.

Matlab Wavelet Toolbox User's Guide, http://www.mathworks.com/access/helpdesk/help/pdf_doc/wavelet/wavelet_ug.pdf.

Pajares, G. and J. M. de la Cruz, 2004. A wavelet-based image fusion tutorial. *Pattern Recognition*, 37 (9): 1855-1872.

Solbø, S. and T. Eltorft, 2004. Homomorphic Wavelet-Based Statistical Despeckling of SAR Images, *Geoscience and Remote Sensing, IEEE Transactions on*, 42(4): 711-720.

Tso, B. and R. C. Olsen, 2005. A contextual classification scheme based on MRF model with improved parameter estimation and multiscale fuzzy line process, *Remote Sensing of Environment*, 97(1): 127-136.

Yoo, H. Y., K. Lee, and B. D. Kwon, 2007. Application of the 3D Discrete Wavelet Transformation Scheme to Remotely Sensed Image Classification, *Korean Journal of Remote Sensing*, 23(5): 355-363.

Yunhao, C., D. Lei, L. Jing, L. Xiaobing, and S. Peijun, 2006. A new wavelet-based image fusion method for remotely sensed data, *International Journal of Remote Sensing*, 27(7): 1465-1476.